PLANT SCIENCE TODAY
ISSN 2348-1900 (online)
Vol 12(2): 1-10
https://doi.org/10.14719/pst.5933

HORIZON
e-Publishing Group
HePG

RESEARCH ARTICLE

Computational investigations of bio-active phytoconstituents from *Chamaecostus cuspidatus* (Nees & Mart.) C. Specht & D.W. Stev. against peroxisome proliferator-activated receptor gamma (PPARG) protein of type 2 diabetes mellitus

Chandra Sekhar Tripathy[1], Santosh Kumar Behera[2] & Sagarika Parida[1]*

[1]Department of Botany, School of Applied Sciences, Centurion University of Technology and Management, Bhubaneswar 752 050, India

[2]Department of Biotechnology, National Institute of Pharmaceutical Education and Research, Ahmedabad 382 355, India

*Email: sagarika.parida@cutm.ac.in

OPEN ACCESS

ARTICLE HISTORY
Received: 18 October 2024
Accepted: 09 January 2025
Available online
Version 1.0 : 10 April 2025
Version 2.0 : 15 April 2025

Check for updates

Additional information
Peer review: Publisher thanks Sectional Editor and the other anonymous reviewers for their contribution to the peer review of this work.

Reprints & permissions information is available at https://horizonepublishing.com/journals/index.php/PST/open_access_policy

Publisher's Note: Horizon e-Publishing Group remains neutral with regard to jurisdictional claims in published maps and institutional affiliations.

Indexing: Plant Science Today, published by Horizon e-Publishing Group, is covered by Scopus, Web of Science, BIOSIS Previews, Clarivate Analytics, NAAS, UGC Care, etc
See https://horizonepublishing.com/journals/index.php/PST/indexing_abstracting

CITE THIS ARTICLE
Chandra Sekhar T, Santosh Kumar B , Sagarika P. Computational investigations of bio-active phytoconstituents from *Chamaecostus cuspidatus* (Nees & Mart.) C. Specht & D.W. Stev. against peroxisome proliferator-activated receptor gamma (PPARG) protein of type 2 diabetes mellitus. Plant Science Today. 2025; 12(2): 1-10. https://doi.org/10.14719/pst.5933

Abstract

Abnormalities in the body's propensity to control and take advantage of sugar as fuel result in type 2 diabetes mellitus (T2DM). Targeting the transcription factor peroxisome proliferator-activated receptor gamma (PPARG) protein, which controls the expression of proteins critical to the progression of type 2 diabetes mellitus (T2DM), is an intriguing approach for treating T2DM. Therefore, the current study focuses on predicting more effective natural compounds for better treatment. *Chamaecostus cuspidatus* (Nees & Mart.) C. Specht & D. W. Stev. belonging to the family *Costaceae*, traditionally acknowledged as an insulin herb, has been taken for the study. Phytocompounds were collected from the published literature, followed by *in silico* ADMET toxicity checking and molecular docking study against the PPARG protein at its specific binding sites. A quantum computation study was performed to check the reactivity of the ligands and normal mode analysis (NMA) was employed to study and characterize the selected protein's flexibility and stability with network analysis. Anti-diabetic drug Biguanide (Metformin) was taken as a standard drug. From this study, Kaempferol resulted with a premier imperative affinity of -7.1 kcal/Mol, with the lowest band gap energy that forms one conventional hydro bond with His466, which is suggested as a new drug molecule for T2DM treatment. In molecular dynamics simulation, the natural compound Kaempferol reflected better stability with the target protein PPARG.

Keywords

molecular docking; molecular dynamics simulation; normal mode analysis; quantum chemical calculation; type 2 diabetes mellitus

Introduction

A perilous, chronic disease with many complications, type 2 diabetes mellitus (T2DM) is the most prevalent cause of illness in the globe. Due to an absolute or relative deficiency of the hormone insulin, this metabolic circumstance is represented by hyperglycaemia and abnormalities in the metabolism of carbohydrates, proteins and fats. Targeting the transcription element peroxisome proliferator-activated receptor gamma (PPARG), which tiller the biosynthesis of T2DM-related proteins, is an intriguing approach for treating T2DM (1). Having many roles in metabolism, especially glucose equipoise, which is dysfunctioning in T2DM, PPARG activity is essential for the emergence and prevalence of T2DM. The oversight of adipogenesis in white adipose tissue is one of PPARG's key roles; in fact, PPARG is both obligatory and competent for

morphing fibroblastic precursors into adipocytes (2, 3). Adiponectin, leptin, TNF-, IL-6 and resisting are just a few of the cytokines and adipokines secreted by fatty tissues (4). These pro-inflammatory chemicals significantly impact the onset of insulin resistance and obesity (5). Although PPARG is found in the liver and muscle, which substantially impacts insulin sensitivity, its roles are most prominent in white adipose tissue, where the receptor is most abundantly expressed. PPARG serves as a promising avenue for therapy for the remedy and stewardship of T2DM due to its crucial involvement in developing T2DM. T2DM has become a global disease, so much research has been conducted worldwide to treat this disease with satisfactory results. This investigation also focuses on the PPARG protein, which is a vital protein involved in T2DM to stop the overexpression of this protein with the help of natural compounds.

Organic compounds of biological genesis that undergo formation by a plant's cells are known as phytoconstituents. Biosynthesis is the process by which plants can transform simple chemical components into intricate organic compounds with the assistance of enzymes. There are numerous uses for the isolated or extracted chemical ingredients in medications. Plants are natural sources of organic compounds, are filled with multiple medicinal properties and provide dedicated service to humanity. In the current study, *Chamaecostus cuspidatus* (Nees & Mart.) C. Specht & D. W. Stev. (*Costus igneus*) has been taken as the target plant for the investigation. Southeast Asian native *Costus igneus*, known as the "insulin plant," is a traditional medicine. In India, *C. cuspidatus*, a member of the *costaceae* family, is specified as the "insulin herb" because its leaves enable the body to release more insulin. This traditional plant has recently gained acceptance on a global level and is widely utilized as an Ayurvedic medicinal herb (6). In terms of the plant's anti-diabetic activity, whole plant parts were taken for the study.

In drug development, the current world needs to find faster and more effective solutions to treat a disease and computational drug development plays a vital role in drug design (7). So, the current study focuses on the *in-silico* drug development procedure to predict effective phytocompounds from *C. cuspidatus*, which will better affect PPARG in treating T2DM. In the study, the reported phytocompounds have undergone different screening procedures to identify better phytocompounds for molecular docking against PPARG protein of T2DM. Quantum computation was performed to study the reactivity of the molecules and normal mode analysis (NMA) was conducted to examine the dynamics and characterize the selected protein's flexibility and stability and predict large amplitude motions. Network analysis was performed to identify the hub genes associated with PPARG protein of T2DM. The molecular dynamic simulation study was performed to analyze the stability of protein-ligand complexes.

Materials and Methods

Sequence, structure and functional annotation

The UniProt database was employed to retrieve the target PPARG gene's sequence, structural specifics and functional particulars (8). The experimental structure of the PPARG protein of T2DM was recovered from the Protein Data Bank (PDB) (9).

Retrieval of phytoconstituents

In this study, twenty-five phytoconstituents of *C. cuspidatus* were selected by searching their information in various published literature (10-13). These biochemical configurational particulars were procured from the PubChem database (14) in SDF format. Using the Biovia Discovery Studio 2021 (15) version, the 3D structures were transformed into PDB format.

Lipinski's rule of five and toxicity studies

Lipinski's rule of five (16) indicates that an internally administered medicine is required to abide by the specifications of molecular mass (<=500 D), logP (<=5), hydrogen bond donor (<=5), hydrogen bond acceptors (<=10) and molar refractivity (40–130), is the most crucial criterion for picking out a medication. If specifications are unmet, a molecule has no significance as a drug-Lipinski's Rule of Five anticipated by the TarGetNet Server (17). The ligands were classified utilizing Lipinski's Rule of Five and were further investigated for their toxicity using Protox-II (18). The tool's control was left in its pre-set configurations.

Prediction of binding site

The Computed Atlas of Surface Topography of Proteins (CASTp) web server (19) assessed the binding vicinity of selected PPARG proteins identified as a target for T2DM. It was determined that most outcomes identified active amino acid residues that portrayed the phytoconstituents' binding region.

Molecular docking of screened phytoconstituents against selected target protein of T2DM

The AutoDock vina tool (20, 21) was utilized in the work above for molecular docking studies to identify the ailment target protein to more appropriately juxtapose the target disease T2DM.

Density Functional Theory (DFT) analysis

A quantum computer simulation was executed using a presumption from Density Functional Theory (DFT) to assess the reactivity and potency of the practicable ligands mobilized in this research. Leveraging the Becke 3-parameter Lee-Yang-Parr (B3LYP) correlation operation of DFT, the reactivity and efficacy have been monitored (22). The DFT analysis was implemented to ascertain the energies of the highest occupied molecular orbital (HOMO) and lowest unoccupied molecular orbital (LUMO) for the organic molecules with the optimal interacting scores and therapeutics that are readily available (standard) commercially for the various targeted disorders. With the assistance of the ORCA Program's version 4.0, the vitality has been established (23).

Protein-protein interaction network analysis of PPARG protein

Understanding protein-protein interactions (PPIs), critical to practically aggregate exertion in a cell in both flourishing and ailing conditions, is indispensable for compassionating cell morphology. Due to the potential adverse effects of pharmacon on PPIs, it is also decisive for medicament augmentation. The biological interactions between proteins in a cell can be illustrated empirically by PPI networks. The STRING database (24) was employed to predict the interconnection of PPARG protein with other proteins.

Normal mode analysis (NMA)

The flexible state a protein can access around equilibrium premises can be summed up with NMA. Numerous articles have focused on the utilization of NMA to study biological macromolecules and it has been reliably demonstrated that these states have functional vitality. Advances in computer technology and normal mode estimation algorithms have made NMA one of the least computationally expensive approaches to discovering the dynamics of macromolecules. The technique known as normal mode analysis can be utilized to define the flexible states that a protein or other molecule can access around a place of equilibrium (25). The Imods server has been employed to study the dynamics behavior of this PPARG protein of T2DM (26).

Molecular dynamic simulation

Molecular dynamics (MD) is a method of complex algorithms to study and foresee the motions of atoms and molecules in a hierarchy of macromolecular structure-to-function coincidences. MD is a process that employs complex algorithms to investigate and anticipate the motions of atoms and molecules in a hierarchy of macromolecular structure-to-function coincidences (27). By providing the atoms and molecules with a set limit on time to interact, the dynamic "evolution" of the entire structure is exemplified (28). The Desmond program (Schrödinger Release 2022-4: Maestro, Schrödinger, LLC, New York, NY, 2022) was used to do MD simulations in Apo (only protein) of PPARG protein of T2DM. In Holo states of PPARG protein complexed with 2 ligands, those are Holo1: PPARG-Kaempferol complex and Holo2: PPARG-Biguanide complex. After a 100 nanosecond (ns) molecular dynamics simulation, the ligand-protein complexes that performed the highest were assessed within the MD paradigm, where the steps were minimization, heating, equilibration and manufacturing (29). Instinctively, topology was reached by establishing the OPLS4 force field and efficiently minimizing atomic coordinates and protein-ligand interactions regarding energy (30). The SPC solvent model was used for immersing the compound in an asymmetrical box of 15 × 15 × 10 Å. By adding 0.15 M NaCl, the physiological pH was annihilated. The water box was configured using the Particle Mesh Ewald (PME) boundary circumstances, ensuring no solute atoms are found below 10 Å of the frontier. Employing the NPT combination, the entire structure was simulated for 100 ns at 300 K. Plots of root mean square fluctuation (RMSF) and deviation (RMSD) were used to look into the dynamic behavior and changes to the structure of the proteins. RMSD assesses the variance in a protein's backbones between their initial and final assignments, highlighting the fraction of the protein or complex that has become flexible (31, 32). The simulated interaction graph can determine the most likely pattern for ligand interactions at the protein attachment site (33, 34).

Results

Sequence and structural information retrieval of PPARG Protein

The target protein was searched in the UniProt database to get its detailed information. It was found that PPARG Protein had P37231 UniProt id with an amino acid (aa) length of 505 aa. The PDB id 2QMV taken for the study was determined using NMR with sequence lengths 235 to 504. The detailed information is given in Table 1.

Phytochemicals of C. cuspidatus

Twenty–five phytochemicals of *C. cuspidatus* were retrieved from reported published research articles. Table 2 gives detailed information regarding the 25 phytochemicals. Their details were obtained from the PubChem database.

Lipinski's rule of five and toxicity annotation

Target Net's web server was used to apply the Lipinski rule of five, which eliminated 18 of the 25 ligands that fulfilled all the criteria. Table 3 depicts the results. The 18 did not abide by this criterion because they did not give 100% results, which reflects that these compounds do not follow Lipinski's rule of 5 completely. Only 7 compounds were found following the Lipinski rule completely. These 7 compounds were further screened through the Protox-II server for toxicity checking and consensus results were prepared that the 7 compounds were found to follow Lipinski's rule of five completely and were nontoxic. This analysis identified 7 compounds that qualified for further molecular docking analysis (Table 4).

Table 2. Description of retrieved phytoconstituents of *C. cuspidatus*

Sl. No.	Chemical name	Molecular formula	PMID
1.	12-Octadecadienoic acid	$C_{18}H_{32}O_2$	129630222
2.	Alpha-Tocopherol	$C_{29}H_{50}O_2$	14985
3.	alpha-ionone	$C_{13}H_{20}O$	5282108
4.	Ascorbic acid	$C_6H_8O_6$	54670067
5.	Beta-carotene	$C_{40}H_{56}$	5280489
6.	Beta-ionone	$C_{13}H_{20}O$	638014
7.	Corosolic acid	$C_{30}H_{48}O_4$	6918774
8.	Dodecanoic acid	$C_{12}H_{24}O_2$	3893
9.	Diosgenin	$C_{27}H_{42}O_3$	99474
10.	Ethyl oleate	$C_{20}H_{38}O_2$	5363269
11.	Farnesylacetone	$C_{18}H_{30}O$	1711945
12.	Kaempferol	$C_{15}H_{10}O_6$	5280863
13.	Gracillin	$C_{45}H_{72}O_{17}$	159861
14.	Hexadecanoic acid	$C_{16}H_{32}O_2$	985
15.	Lupenol	$C_{30}H_{50}O$	259846
16.	Myristic acid	$C_{14}H_{28}O_2$	11005
17.	Octadecanoic acid	$C_{18}H_{36}O_2$	5281
18.	Oleic acid	$C_{18}H_{34}O_2$	445639
19.	Oleyl alcohol	$C_{18}H_{36}O$	5284499
20.	Quercetin	$C_{15}H_{10}O_7$	5280343
21.	Sitosterol	$C_{29}H_{50}O$	222284
22.	Squalene	$C_{30}H_{50}$	638072
23.	Stigmasterol	$C_{29}H_{48}O$	5280794
24.	Tetradecanoic acid	$C_{14}H_{28}O_2$	11005
25.	Tigogenin	$C_{27}H_{44}O_3$	99516

Table 1. PPARG protein information of T2DM

Sl. No.	Entry Id (UniProt)	Protein Name	Gene Name	Amino acid Length	PDB ID taken for study
1.	P37231	Peroxisome proliferator-activated receptor gamma	PPARG	505	2QMV NMR (235-504)

Table 3. Lipinski's rule of five analyses of the phytoconstituents of *C. cuspidatus*

Sl. No.	Phytochemicals Name	MR (Molar Refractivity) (40-130)	Molecular weight (<=500 D)	HBD (H-bond Donor) (<=5)	HBA (H- bond Acceptors) (<=10)	LogP (<=5)	Lipinski's rule of five
1.	12-Octadecadienoic acid	89.4638	280.44548	1.0	2.0	5.8845	75%
2.	Alpha-tocopherol	139.271	430.7061	1.0	2.0	8.8402	75%
3.	alpha-ionone	61.483	192.2973	0.0	1.0	3.5141	100%
4.	Ascorbic acid	35.1202	176.12412	4.0	6.0	-1.4074	100%
5.	Beta-carotene	184.432	536.87264	0.0	0.0	12.6058	50%
6.	Beta-ionone	61.483	192.2973	0.0	1.0	3.6582	100%
7.	Corosolic acid	138.0754	472.69972	3.0	4.0	6.0603	75%
8.	Dodecanoic acid	61.5698	200.31776	1.0	2.0	3.9919	100%
9.	Diosgenin	121.5948	414.62058	1.0	3.0	5.7139	75%
10.	Ethyl oleate	99.065	310.51452	0.0	2.0	6.587	75%
11.	Farnesylacetone	87.418	262.4302	0.0	1.0	5.7748	75%
12.	Kaempferol	76.012	286.2363	4.0	5.0	2.2824	100%
13.	Gracillin	217.5832	885.04298	9.0	17.0	0.2141	25%
14.	Hexadecanoic acid	80.7978	256.42408	1.0	2.0	5.5523	75%
15.	Lupenol	135.1418	426.7174	1.0	1.0	8.0248	75%
16.	Myristic acid	71.1838	228.37092	1.0	2.0	4.7721	100%
17.	Octadecanoic acid	90.4118	284.47724	1.0	2.0	6.3325	75%
18.	Oleic acid	89.9378	282.46136	1.0	2.0	6.1085	75%
19.	Oleyl alcohol	89.3278	268.47784	1.0	1.0	6.0162	75%
20.	Quercetin	78.035	302.2357	5.0	6.0	1.988	75%
21.	Sitosterol	133.2288	414.7067	1.0	1.0	8.0248	75%
22.	Squalene	143.48	410.718	0.0	0.0	10.605	75%
23.	Stigmasterol	132.7548	412.69082	1.0	1.0	7.8008	75%
24.	Tetradecanoic acid	71.1838	228.37092	1.0	2.0	4.7721	100%
25.	Tigogenin	122.0688	416.63646	1.0	3.0	5.7938	75%

Binding site prediction of PPARG protein

The PDB id 2QMV of PPARG Protein taken for the study was uploaded in the CastP web tool to depict the imperative spots. The binding sites for PPARG protein are Lys263, Phe264, Lys265, His266, Ile267, Thr268, Leu270, Ser274, Lys275, Ile279, Gln283, Ser464, Leu465, His466 and Leu468. Fig. 1 represents the area predicted by the CastP server as binding sites.

Molecular docking study

In computer-assisted therapeutic discovery and structural molecular biology, molecular docking is crucial. Finding the dominant binding mode(s) of a ligand with a protein with an acknowledged 3D structure is the primary objective of ligand-protein docking interaction. In the current docking simulation approach, the AutoDock tool obtains the results throughout the docking process. AutoDock 4.2 tool is used to determine the grid box. Kollman charges were initially allotted to the selected protein. Subsequently, Gasteiger partial charges were delegated to the inhibitors above. The grid box was prepared according to the predicted binding sites of the PPARG protein. The grid box value was found with the coordinates X -62, Y - 56 and Z -66. After obtaining the grid box value, AutoDock Vina was employed to do the molecular docking studies. Here, the highly reported compound Biguanide is standard (35). It was obtained that Kaempferol was found with preeminent interacting affinity of -7.1 kcal/Mol and forming Hydrogen bonding with His466 followed by Beta-Ionone with second apical with docking affinity of -6.0 kcal/Mol and Myristic acid with third maximal with interacting score of -5.9 kcal/Mol. In contrast, the standard drug Biguanide showed only an interacting score of -4.7 kcal/Mol. Table 5 depicts the docking repercussions. Fig. 2 & 3 represent the 2D and 3D molecular reciprocation of 7 selected molecules of *C. cuspidatus* and Biguanide with PPARG protein.

Quantum chemical calculation

Due to quantum computation's crucial nature, quantum chemistry was analysed to learn about frontier molecular descriptors for 7 intended molecules and the reported escalate Biguanide (Table 6), where Kaempferol displayed the lowest gap energy followed by Beta-ionone. Besides descriptors entailed, HOMO (highest occupied molecular orbital) and LUMO (lowest unoccupied molecular orbital), Electronic Energy (eV), Potential Energy (eV), Kinetic Energy (eV) and Dipole Moment (Debye). The compelling acuteness for Kaempferol and Beta-ionone compounds, found with band energy gap (ΔE), i.e., the difference between $_{E}$LUMO and $_{E}$HOMO, with appraises 10.883 and 10.855 eV. Kaempferol and Beta-ionone displayed higher acuteness when compared to Biguanide, based on its slightest band energy gap. Fig. 4 represents the DFT results for Kaempferol, Beta-ionone and Biguanide.

Network analysis

PPARG gene undergoes a STRING database to search for interlinked genes. Table 7 depicts the results in detail. Here, the parameter in STRING databases is set with no. of nodes, i.e., 20, to predict highly associated genes with PPARG protein. Fig. 5 represents the genetic interaction network of the PPARG protein with other proteins. The line joining nodes in different colours represents distinct interactions: Blue line: compiled from database curation: the experimentally established represented through magenta line: Gene neighbourhood is portrayed by the green line: Red line: Fusion of genes Indigo blue line: co-occurrence of genes Light green line: mining text Line: in black: co-expression: homology proteins reflected by light blue.

Table 4. Toxicity analysis of the selected phytoconstituents from *C. cuspidatus* using Protox-II Server

Sl. No.	Phytochemical compound	Toxic /Non-Toxic
1.	alpha-ionone	Non-Toxic
2.	Ascorbic Acid	Non-Toxic
3.	Beta-Ionone	Non-Toxic
4.	Dodecanoic acid	Non-Toxic
5.	Kaempferol	Non-Toxic
6.	Myristic Acid	Non-Toxic
7.	Tetradecanoic acid	Non-Toxic

Table 5. Molecular docking results of seven selected phytoconstituents from *C. cuspidatus* and reported compound Biguanide against Peroxisome proliferator-activated receptor gamma (PPARG) protein of T2DM

Sl. No.	Phyto-compound	Binding Energy scores (kcal/Mol)	No. of Hydrogen Bonds	Hydrogen-Bond forming residues
1.	Alpha-ionone	-5.8	-	-
2.	Ascorbic Acid	-4.6	4	Lys358, Gly361, Lys354, Leu356
3.	Beta-Ionone	-6.0	-	-
4.	Dodecanoic acid	-5.3	2	Arg288, Gly284
5.	Kaempferol	-7.1	1	His466
6.	Myristic Acid	-5.9	2	Lys263, Arg280
7.	Tetradecanoic acid	-5.2	1	Arg288
8.	Biguanide (marketed)	-4.7	2	Cys285, Leu340

Table 6. DFT results of best phytocompound selected from *C. cuspidatus* showing better result against PPARG protein target of T2DM and reported compound Biguanide

Sl. No.	Phytochemical name	Electronic Energy (eV)	Potential Energ (eV)	Kinetic Energ (eV)	LUMO (eV)	HOMO (eV)	GAP Energy (eV)	Dipole Moment (Debye)
1.	Alpha-ionone	-40560.26672	-31389.91912	15652.27241	2.465	-9.224	11.689	3.18894
2.	Ascorbic Acid	-39235.06521	-36968.14397	18451.50534	2.884	-9.660	12.544	5.23384
3.	Beta-Ionone	-40563.12303	-31393.51223	15655.99180	2.171	-8.684	10.855	3.75369
4.	Dodecanoic acid	-39370.72151	-33532.24735	16723.61894	4.615	-11.564	16.179	1.75371
5.	Kaempferol	-70771.00004	-55518.42058	27702.09500	2.141	-8.742	10.883	4.63190
6.	Myristic Acid	-46049.37423	-37765.48782	18833.99770	4.615	-11.497	16.112	1.77664
7.	Tetradecanoic acid	-46049.37423	-37765.48782	18833.99770	4.615	-11.497	16.497	1.77664
8.	Biguanide (reported)	-17810.66493	-19095.38413	9522.56036	4.681	-8.816	13.497	1.74138

Table 7. Genetic network interaction analysis of PPARG protein selected in the study of T2DM using STRING Database

Genetic interaction observation	STRING NETWORK
	PPARG
Number of Nodes	21
Number of Edges	149
Average Node Degree	14.2
Avg. Local Clustering Coefficient	0.85
Expected Number of Edges:	48
PPI Enrichment P-Value	< 1.0e-16
Genes interacted	PRDM16, XPR1, KDM3A, PAX8,CTNNB1, RELA, NCOR2, NCOA2,FABP4,MED1,NCOA1,SREBF1,PPARGC1A, SIRT1,RXRA,EP300,CREBBP,CEBPA,NCOR1,CEBPB

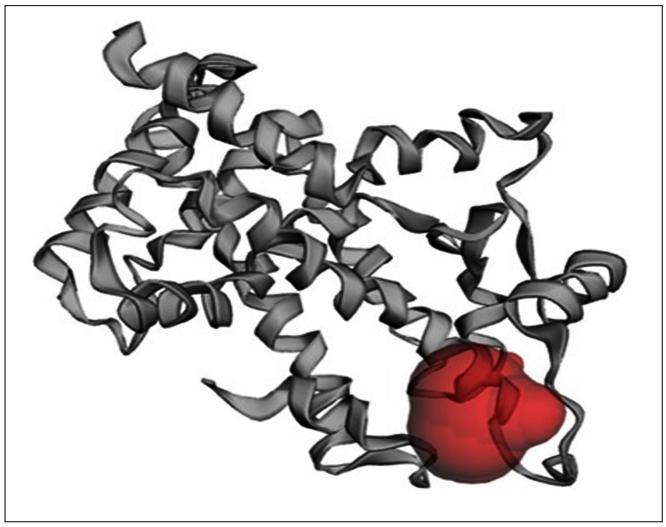

Fig. 1. Predicted area of binding region of PPARG Protein.

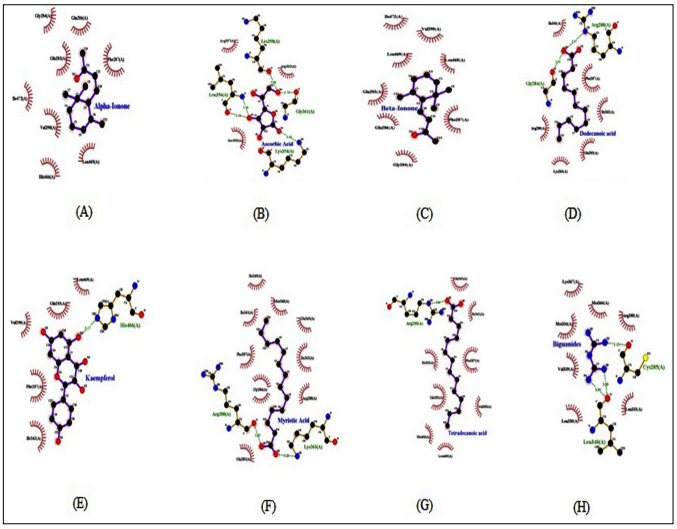

Fig. 2. Molecular docking 2D-interaction of (A) PPARG Protein-Alpha-Ionone (B) PPARG Protein- Ascorbic Acid (C) PPARG Protein- Beta-ionone (D) PPARG Protein-Dodecanoic acid (E) PPARG Protein- Kaempferol (F) PPARG Protein-Myristic acid (G) PPARG Protein- Tetradecanoic acid (H) PPARG Protein-Biguanide. Visualized using LigPlot + tool.

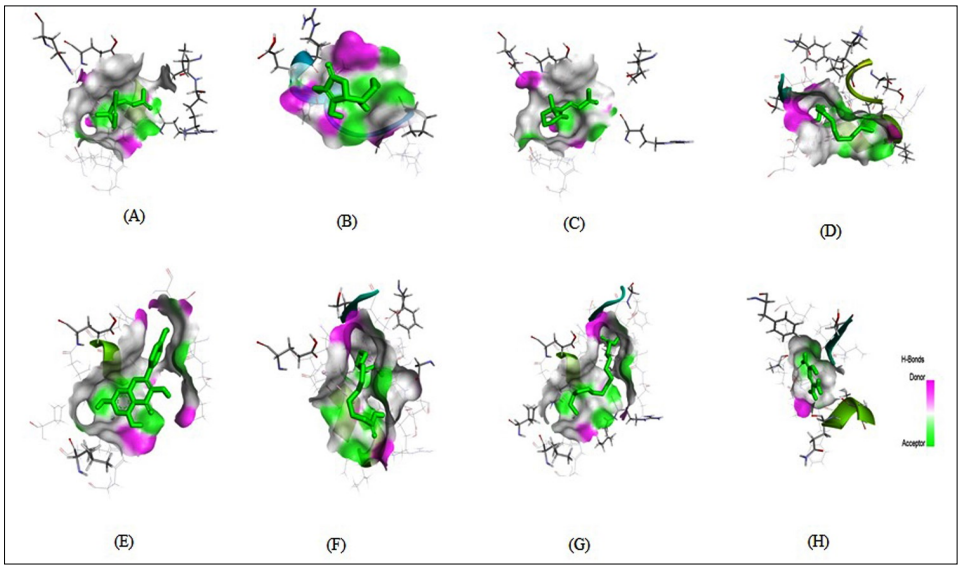

Fig. 3. Molecular docking 3D-interaction of (A) PPARG Protein-Alpha-ionone (B) PPARG Protein- Ascorbic acid (C) PPARG Protein- Beta-ionone (D) PPARG Protein-Dodecanoic acid (E) PPARG Protein- Kaempferol (F) PPARG Protein- Myristic acid (G) PPARG Protein- Tetradecanoic acid (H) PPARG Protein- Biguanide. Visualized using Biovia Discovery studio tool.

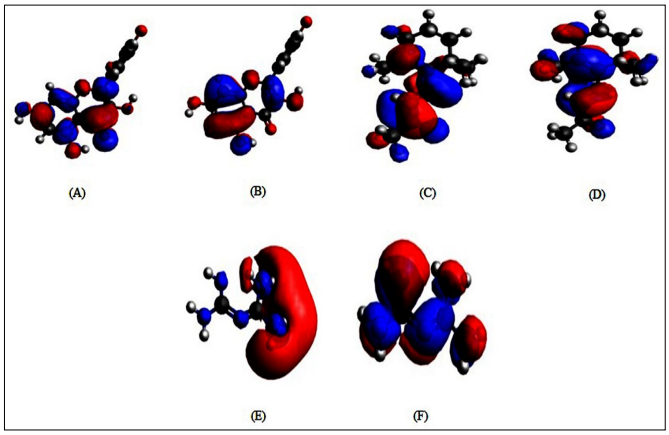

Fig. 4. DFT results: (A) LUMO- Kaempferol (B) HOMO- Kaempferol (C) LUMO-Beta-ionone (D) HOMO- Beta-ionone (E) LUMO- Biguanide (F) HOMO-Biguanide. The positive and negative electron densities are connoted by red & blue color.

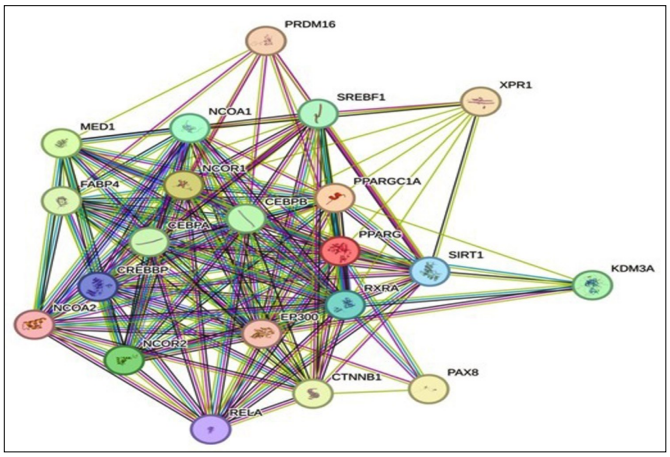

Fig. 5. Interaction network of PPARG protein with other proteins.

Normal mode analysis (NMA)

Using the iMODS server to quantify the B-factor (a protein's atom disorder), calculate eigenvalue and monitor structural deformability, the normal mode analysis method was utilized to determine the PPARG protein's substantial movement and stability. Fig. 6 gives the results of NMA. In Fig. 6 (A), the Deformability B-factor is viewed and found with lesser no. of peaks and in Fig. 6 (B), the Mobility B-factor is viewed and obtained that the NMR structure taken for the study does not vary with the NMA structure. Fig. 6 (C) gives the Eigenvalue value of 2.382481e-04. In Fig. 6 (D), the variance is illustrated. In Fig. 6 (E), the covariance matrix is embellished with the pictograph adumbration (via white, red and blue colours). Colour modulation insinuates the analogous, differentiable and anti-parallel couplets of amino acid residues. Fig. 6 (F) gives the elastic network model and springs of atomic acquaintance are ordained as grey dots in the miniature, where the callousness of reciprocal action to the acclivity of the grey colour.

Assessment of molecular dynamics simulation trajectories

The highly complex MD algorithm addressed the relationships between atoms and molecules in a system of physical relationships between macromolecular elements and their roles. The multifaceted evolution of the system was apparent in permitting the atoms and molecules to interact for an allocated amount of time. A 100 ns molecular dynamics simulation, including structural rearrangements of molecules and receptors, was undertaken to assess the docked complex's stability. The dynamics and stability of Apo and Holo systems (PPARG: Apo; Holo1: PPARG-Kaempferol complex, Holo2: PPARG -Biguanide complex were evaluated using Desmond suit, to figure out the dynamic behaviour and bonding mechanism. For PPARG protein, the dynamic rigidity of both systems (Apo and Holo) was evaluated by adopting the RMSD profile of the backbone atoms at 100 ns. Fig. 7 displays results. The backbone RMSD graph of Holo1 state: PPARG - Kaempferol complex revealed a stable RMSD during ~35 to 70 ns compared to its Apo state with values between ~2.8 to ~4.0 Å in the initial stage and after that second stable RMSD found during ~75 ns to 85 ns with its value between ~3.0 to 4.0 defining a stable configuration throughout 100 ns simulation process, whereas in Holo2: PPARG -Biguanide complex conveyed smaller stable RMSD during ~75 to 85 ns and rest unstable avenues throughout the simulation cycle upon comparison to its Apo state MD simulations with higher fluctuation picks defining the instability nature. The backbone atoms' RMSD profile at 100 ns is presented in Fig. 7, illustrating the dynamic stability of both the Apo and Holo systems for ligands establishing complexes

with the PPARG protein. Taking together the RMSD values of all 2 Holo states in the case of PPARG, Holo1 revealed minor deviations and a stable trajectory, followed by Holo2. This depicts that the compound Kaempferol could inhibit the PPARG and aid in maintaining rigidity by tailoring its molecular framework compared to Biguanide.

Further validation for the RMSD result emerged from root mean square fluctuation (RMSF), which quantifies residue variability. The dispersion among various residues has been monitored in each state implementing RMSF plots. Thus, comparable to the Holo states, the Apo state observed more extensive fluctuations for PPARG protein, demonstrating the simulation's constrained motions. For Holo1, the amino acid residues between 45 to 75 and 130 to 145 displayed significant variations within their Cα atoms contrary to alternate locations. For Holo2, a constant variation was observed between 25 to 30, 70 to 80 and 125 to 140. The fluctuations could be due to various interactions. Protein residues that interact with the ligand are marked with green-colour vertical bars. The findings confirm that ligand binding could render residues in the Holo state more stationary than in the Apo state. Fig. 8 depicts the RMSF results.

H-bond analysis

Schrödinger Release 2022-4 was utilized in MD simulations to illustrate intermolecular hydrogen bonds, identifying variables and determining the stability of the drug-target complex. The intermolecular hydrogen bonds of the Holo states were tracked. The stacked bar chart of Holo1 in Fig. 9 (A) shows that amino acid residues of Post MD PPARG-Kaempferol complex intermolecular Hydrogen bonds formed with Leu255, Glu259, Arg280, Gln283, Ile341, Glu343, Gly344 and Gly346 may play a vital role in the binding and regulation of the protein. In the case of the Holo2 state in Fig. 9 (B) for PPARG-Biguanide Post MD complex intermolecular Hydrogen bonds formed with Glu291, Glu295 and Glu343, which defines Biguanide has less stability with PPARG. Fig. 9 depicts the results.

The simulation of the Holo1 state (PPARG-Kaempferol complex) represented a consistent number and intensified intermolecular hydrogen bonds throughout the simulation with lesser deviation, whereas the Holo2 state (PPARG-Biguanide complex) has inconsistent H-bonds. Fig. 10 shows the results for the stabilized hydrogen bonding interactions in post MD protein-ligand interaction of all the Holo states.

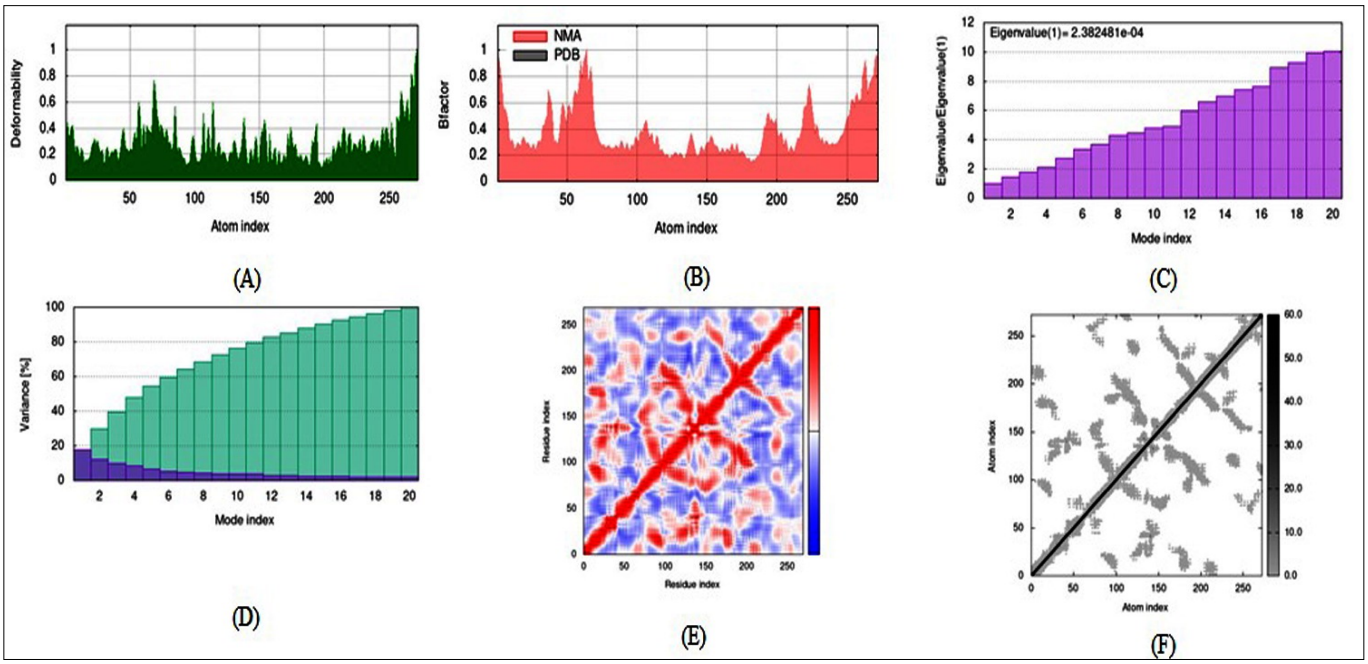

Fig. 6. Normal mode analysis of PPARG Protein (A) Deformability B-factor (B) Mobility B-factor (C) Eigenvalue (D) Variance (E) Co-variance (F) Elastic network.

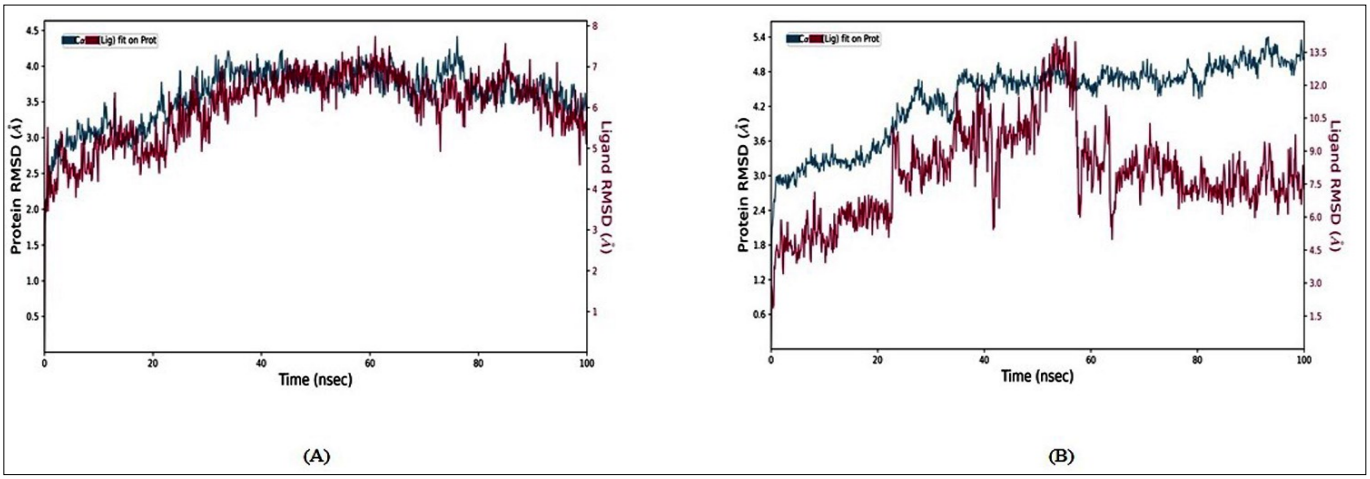

Fig. 7. The structural rigidity of the Apo and Holo states of PPARG protein throughout 100 nanoseconds (ns) time period of MDS Backbone-RMSD (a) PPARG-Kaempferol complex (b) PPARG -Biguanide complex.

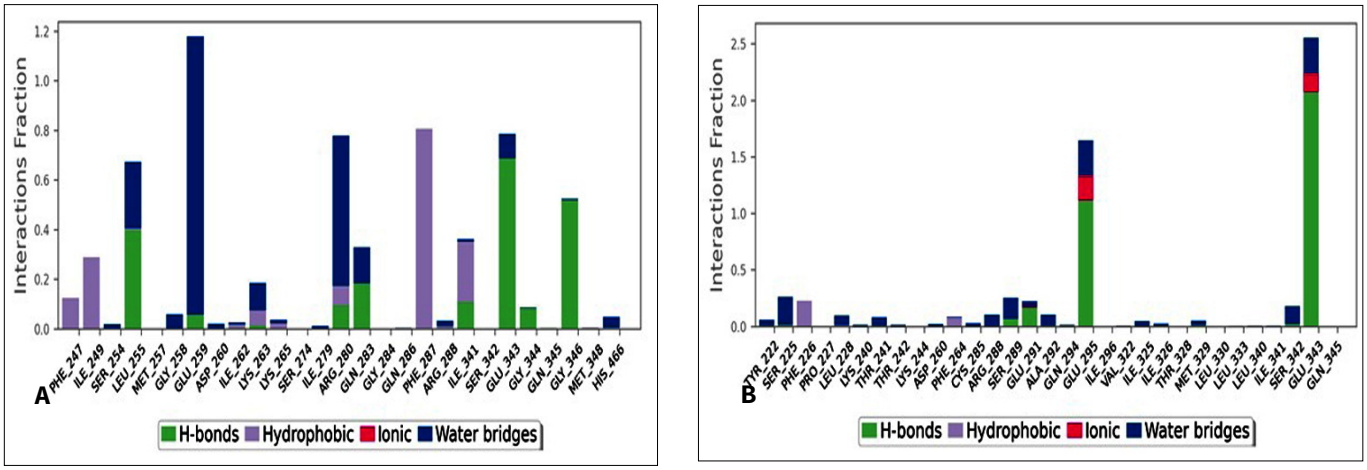

Fig. 9. Stacked bar chart plot showing protein ligand contacts during the simulation of 100 ns for (A) PPARG-Kaempferol complex (B) PPARG -Biguanide complex.

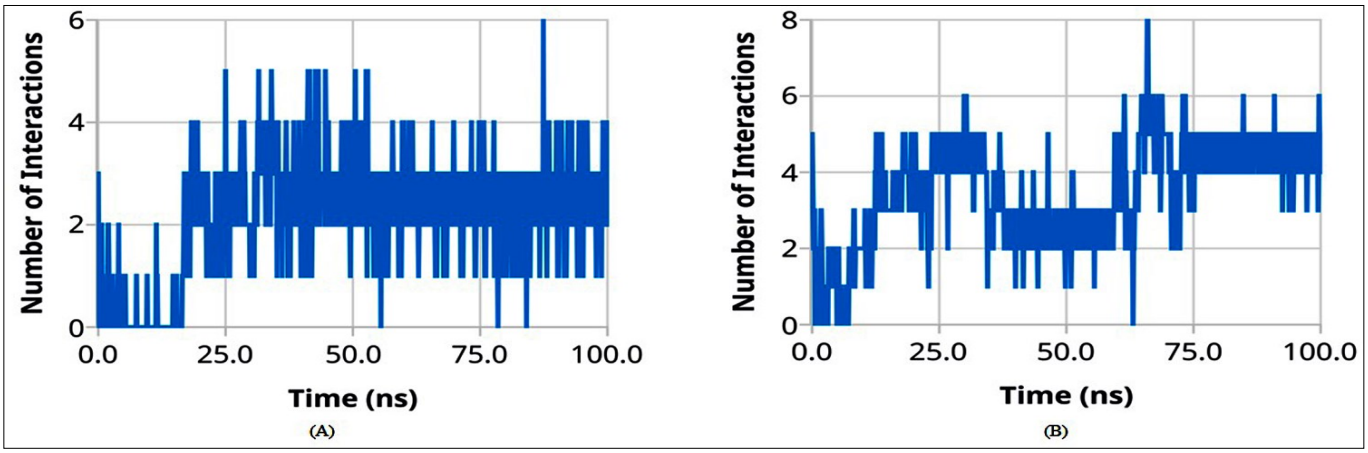

Fig. 10. Stacked bar chart plot showing protein ligand contacts during the simulation of 100 ns for (A) PPARG-Kaempferol complex (B) PPARG -Biguanide complex.

Discussion

Hyperglycaemia is a medical disorder associated with diabetes, which is characterized by elevated blood sugar levels. People from both industrialized and developing nations suffer from T2DM (36) and its implications, which is a universal public health burden. PPARG protein is currently of interest to researchers due to its association as the vital target for T2DM therapeutics (1). Metformin (Biguanide) is the most prescribed drug around the globe as first-line drug well known for managing T2DM by decreasing hepatic glucose production, but it has no role in uprooting T2DM. The genetic linkage of the PPARG gene with other genes may lead to complications and make way for the initiation of other associated diseases inside the human body. Therefore, researchers are on their way to explore potential compounds from natural sources, including *C. cuspidatus*, which is regarded as an insulin plant, for better pharmacotherapeutics in T2DM (7). Concerning the importance of insulin plant, the current investigation implied computer-assisted drug discovery process, involving combinatorial approach of pharmacokinetic studies, molecular docking and DFT analysis, to explore effective anti-diabetic phytochemicals. The *In-silico*, pharmacokinetic studies revealed 7 compounds, namely alpha-ionone, ascorbic acid, beta-ionone, dodecanoic acid, kaempferol, myristic acid and tetradecanoic acid. Subsequently, the molecular docking studies depicted Kaempferol and Beta-ionone with better docking scores compared to others. This finding is well aligned with the existing reports, where Kaempferol has been well appreciated as an anti-diabetic drug and its complications (37). The binding energy of Kaempferol proves its potency to act as a better drug against the PPARG gene and can reduce blood sugar levels by helping the pancreatic Beta-cells for more amount of insulin production.

With its broadened processing power over traditional approaches, quantum computing has the potential to fundamentally change an extensive variety of scientific fields, including medicine. However, proof-of-concept studies have been the main use of quantum computer technology for drug discovery. Through the quantum chemical calculation study, the DFT method was applied to study the reactivity, where screened natural molecules showed the highest reactivity due to lower band gap energy, which defined their faster rate reaction in the side body with better efficacy. The 2 high-scoring compounds Kaempferol and Beta-ionone have the lowest band energy as compared to the other natural compounds and the standard drug Biguanide. The low energy gap of Kaempferol also defines the higher stability of the molecule and strength of binding to the target protein PPARG.

Subsequently, on the other hand, the Normal mode analysis method was applied to check the PPARG protein's stability, flexibility and correlation with Kaempferol. In molecular dynamic simulation, the Kaempferol-PPARG complex resulted highly stable trajectory with higher number of H-bonding residues in post MD simulation interaction defining its stronger attachment than the standard drug. The findings of this *in-silico* study could be employed as evidence for further *in-vitro* and *in-vivo* assessments that are required to validate anti-diabetic medication potency and effectiveness of the compounds against PPARG protein.

Conclusion

The number of patients with T2DM is increasing daily and specific proteins like PPARG play an essential role in rapid growth. In the current study *in silico* drug design process is applied to search for a better phytochemical from *C. cuspidatus*. Here, the compounds Kaempferol and Beta-ionone scored better with reactivity. This computational investigation leads these molecules to further in vitro analysis and development of possible drug candidates to manage T2DM.

Acknowledgements

We appreciate the permission to conduct the study and the support provided by Centurion University of Technology and Management, Odisha, India and the National Institute of Pharmaceutical Education and Research, Ahmedabad, India.

Authors' contributions

CST did data collection, computational work, manuscript preparation, formatting and writing. SKB helped in data collection, computational analysis and writing. SP designed the work and conceived for manuscript writing, correction and analysis. All authors read and approved the final manuscript.

Compliance with ethical standards

Conflict of interest: Authors do not have any conflict of interest to declare.

Ethical issues: None

References

1. Frkic RL, Richter K, Bruning JB. The therapeutic potential of inhibiting PPARγ phosphorylation to treat type 2 diabetes. J Biol Chem. 2021;297(3):101030. https://doi.org/10.1016/j.jbc.2021.101030
2. Lefterova MI, Haakonsson AK, Lazar MA, Mandrup S. PPARγ and the global map of adipogenesis and beyond. Trends Endocrinol Metab. 2014;25(6):293–302. https://doi.org/10.1016/j.tem.2014.04.001
3. Kim HY, Jang HJ, Muthamil S, Shin UC, Lyu JH, Kim SW, et al. Novel insights into regulators and functional modulators of adipogenesis. Biomed Pharmacother. 2024;177:117073. https://doi.org/10.1016/j.biopha.2024.117073
4. Shelake G, Baviskar S, Panda AK, Solankure S, Pandey K, Chauthe S, et al. Exploring the rare variants associated with type 2 diabetes mellitus in Indian population and its disease-drug association studies: an *in-silico* approach. J Biomol Struct Dyn. 2024;42(12):6307–22. https://doi.org/10.1080/07391102.2023.2233634
5. Kawai T, Autieri MV, Scalia R. Adipose tissue inflammation and metabolic dysfunction in obesity. Am J Physiol Cell Physiol. 2021;320(3):C375–91. https://doi.org/10.1152/ajpcell.00379.2020
6. Mathew F, Varghese B. A review on medicinal exploration of *Costus igneus*: the insulin plant. Int J Pharm Sci Rev Res. 2019;54(2):51–57.
7. Bhavsar D, Kutre S, Shikhare P, Kumar S, Behera SK, Chauthe SK. Pharmacoinformatics approach for type 2 diabetes mellitus therapeutics using phytocompounds from *Costus* genus: an *in-silico* investigation. J Biomol Struct Dyn. 2024;1–7. https://doi.org/10.1080/07391102.2024.2330712
8. UniProt Consortium T. UniProt: the universal protein knowledgebase. Nucleic Acids Res. 2018;46(5):2699. https://doi.org/10.1093/nar/gky092
9. Velankar S, Burley SK, Kurisu G, Hoch JC, Markley JL. The protein data bank archive. In: Structural proteomics: High-throughput methods. Humana, New York; 2021. p. 3–21. https://doi.org/10.1007/978-1-0716-1406-8_1
10. Rani D. Phytochemical and pharmacological overview of *Chemoecostus cuspidatus*. Plant Arch. 2019;19(2):4565–73.
11. Shinde S, Surwade S, Sharma R. *Costus Igneus*: Insulin plant and its preparations as remedial approach for diabetes mellitus. Int J Pharm Sci Res. 2022;13:1551–58. https://orcid.org/10.13040/IJPSR.0975-8232.13(4).1551-58
12. Thiruchenduran S, Maheswari KU, Prasad TN, Rajeswari B, Suneetha WJ. UV-Vis scanning coupled with PCA as an alternative method for phytochemical screening of natural products â€“*Costus Igneus* leaf metabolites. J Pharmacogn Phytochem. 2017;6(1):411–16.
13. Nascimento CC, Vasconcelos SD, Camacho AC, Nascimento SF, Oliveira JF, Nogueira RI, et al. A literature review on the medicinal properties and toxicological profile of *Costus spicatus* plant. Res J Life Sci Bioinform Pharm Chem Sci. 2016;2(2):56-68.
14. Kim S, Thiessen PA, Bolton EE, Chen J, Fu G, Gindulyte A, et al. PubChem substance and compound databases. Nucleic Acids Res. 2016;44(D1):D1202–13. https://doi.org/10.1093/nar/gkv951
15. Pawar SS, Rohane SH. Review on discovery studio: An important tool for molecular docking. Asian J Res Chem. 2021;14(1):1–3. https://doi.org/10.5958/0974-4150.2021.00014.6
16. Karami TK, Hailu S, Feng S, Graham R, Gukasyan HJ. Eyes on Lipinski's rule of five: A New “rule of thumb” for physicochemical design space of ophthalmic drugs. J Ocul Pharmacol Ther. 2022;38(1):43–55. https://doi.org/10.1089/jop.2021.0069
17. Yao ZJ, Dong J, Che YJ, Zhu MF, Wen M, Wang NN, et al. TargetNet: a web service for predicting potential drug–target interaction profiling via multi-target SAR models. J Comput Aided Mol Des. 2016;30:413–24. https://doi.org/10.1007/s10822-016-9915-2
18. Banerjee P, Eckert AO, Schrey AK, Preissner R. ProTox-II: a webserver for the prediction of toxicity of chemicals. Nucleic Acids Res. 2018;46(W1):W257–63. https://doi.org/10.1093/nar/gky318
19. Tian W, Chen C, Lei X, Zhao J, Liang J. CASTp 3.0: computed atlas of surface topography of proteins. Nucleic Acids Res. 2018;46(W1):W363–67. https://doi.org/10.1093/nar/gky473
20. Trott O, Olson AJ. AutoDock Vina: improving the speed and accuracy of docking with a new scoring function, efficient optimization and multithreading. J Comput Chem. 2010;31(2):455–61. https://doi.org/10.1002/jcc.21334
21. Mahata S, Behera SK, Kumar S, Sahoo PK, Sarkar S, Fazil MH, et al. *In-silico* and *in-vitro* investigation of STAT3-PIM1 heterodimeric complex: Its mechanism and inhibition by curcumin for cancer therapeutics. Int J Biol Macromol. 2022;208:356–66. https://doi.org/10.1016/j.ijbiomac.2022.03.137
22. Orio M, Pantazis DA, Neese F. Density functional theory. Photosynth Res. 2009;102:443–53. https://doi.org/10.1007/s11120-009-9404-8
23. Neese F. The ORCA program system. WIREs Comput Mol Sci. 2012;2(1):73–78. https://doi.org/10.1002/wcms.81
24. Mering CV, Huynen M, Jaeggi D, Schmidt S, Bork P, Snel B. STRING: a database of predicted functional associations between proteins. Nucleic Acids Res. 2003;31(1):258–61. https://doi.org/10.1093/nar/gkg034
25. Bauer JA, Pavlović J, Bauerová-Hlinková V. Normal mode analysis as a routine part of a structural investigation. Molecules. 2019;24(18):3293. https://doi.org/10.3390/molecules24183293
26. López-Blanco JR, Aliaga JI, Quintana-Ortí ES, Chacón P. iMODS: internal coordinates normal mode analysis server. Nucleic Acids Res. 2014;42(W1):W271–76. https://doi.org/10.1093/nar/gku339
27. Behera SK, Vhora N, Contractor D, Shard A, Kumar D, Kalia K, et al. Computational drug repurposing study elucidating simultaneous inhibition of entry and replication of novel corona virus by

Grazoprevir. Sci Rep. 2021;11(1):7307. https://doi.org/10.1038/s41598-021-86712-2

28. Durrant JD, McCammon JA. Molecular dynamics simulations and drug discovery. BMC Biol. 2011;9:1–9. https://doi.org/10.1186/1741-7007-9-71
29. Raghu R, Devaraji V, Leena K, Riyaz SD, Rani BP, Kumar BS, et al. Virtual screening and discovery of novel aurora kinase inhibitors. Curr Top Med Chem. 2014;14(17):2006–19. https://doi.org/10.2174/1568026614666140929151140
30. Shivakumar D, Williams J, Wu Y, Damm W, Shelley J, Sherman W. Prediction of absolute solvation free energies using molecular dynamics free energy perturbation and the OPLS force field. J Chem Theory Comput. 2010;6(5):1509–19. https://doi.org/10.1021/ct900587b
31. Aier I, Varadwaj PK, Raj U. Structural insights into conformational stability of both wild-type and mutant EZH2 receptor. Sci Rep. 2016;6(1):34984. https://doi.org/10.1038/srep34984
32. Choudhary P, Bhowmik A, Chakdar H, Khan MA, Selvaraj C, Singh SK, et al. Understanding the biological role of PqqB in *Pseudomonas stutzeri* using molecular dynamics simulation approach. J Biomol Struct Dyn. 2022;40(9):4237–49. https://doi.org/10.1080/07391102.2020.1854860
33. Deniz U, Ozkirimli E, Ulgen KO. A systematic methodology for large scale compound screening: A case study on the discovery of novel S1PL inhibitors. J Mol Graph Model. 2016;63:110–24. https://doi.org/10.1016/j.jmgm.2015.11.004
34. Tandon G, Jaiswal S, Iquebal MA, Kumar S, Kaur S, Rai A, Kumar D. Evidence of salicylic acid pathway with EDS1 and PAD4 proteins by molecular dynamics simulation for grape improvement. J Biomol Struct Dyn. 2015;33(10):2180–91. https://doi.org/10.1080/07391102.2014.996187
35. Araki E, Inagaki N, Tanizawa Y, Oura T, Takeuchi M, Imaoka T. Efficacy and safety of once-weekly dulaglutide in combination with sulphonylurea and/or biguanide compared with once-daily insulin glargine in Japanese patients with type 2 diabetes: a randomized, open-label, phase III, non-inferiority study. Diabetes Obes Metab. 2015;17(10):994–1002. https://doi.org/10.1111/dom.12540
36. Sharchil C, Vijay A, Ramachandran V, Bhagavatheeswaran S, Devarajan R, Koul B, et al. Zebrafish: a model to study and understand the diabetic nephropathy and other microvascular complications of type 2 diabetes mellitus. Vet Sci. 2022;9(7):312. https://doi.org/10.3390/vetsci9070312
37. Yang Y, Chen Z, Zhao X, Xie H, Du L, Gao H, et al. Mechanisms of Kaempferol in the treatment of diabetes: A comprehensive and latest review. Front Endocrinol. 2022;13:990299. https://doi.org/10.3389/fendo.2022.990299